Electronic Supplementary Material (ESI) for ChemComm.

Influence of Charge Configuration on Substrate Binding to SARS-CoV-2 Main Protease

ELECTRONIC SUPPLEMENTARY INFORMATION

*Dimas Suárez and Natalia Díaz**

Departamento de Química Física y Analítica. Universidad de Oviedo. Avda. Julián Clavería 8. 33006. Oviedo. SPAIN.

Corresponding Author

* diazfnatalia@uniovi.es. Phone-Number +34-985103468.

Computational Settings

Initial structures and building of the enzyme/peptide complexes

Starting coordinates for the SARS-CoV-2 main protease were taken from the 6LU7[1] (pH=6.0) and 7JUN[2] PDB structures. The coordinates of the inhibitor in 6LU7 were removed prior to the edition. All the crystallographic water molecules were maintained in the models. A heptapeptide (**7-mer**) molecule was placed in the active site of each protomer by means of structure superposition using the 2Q6G crystallographic coordinates as a template. The 2Q6G structure corresponds to the $His_{41}Ala$ mutant of the closely-related SARS-CoV enzyme in complex with a peptide substrate,[3] which mimics the cleavage site between the so-called non-structural protein 4 and the $3CL^{pro}$ enzyme that are successively encoded in the viral polyproteins.[4] In our models, we considered the –Ala_{3260}(P_4)-Val_{3261}(P_3)-Leu_{3262}(P_2)-Gln_{3263}(P_4)~Ser_{3264}(P_1')-Gly_{3265}(P_2')-Phe_{3266}(P_3')– sequence of residues of this recognition site that includes the absolutely conserved glutamine at the P_1 site (*i.e.* cleavage occurs at the P_1~P_1' peptide bond). The peptide molecule was capped with *N*-terminal acetyl- and *C*-terminal *N*-methyl amide groups.

Protonation state and force field representations

Two different protonation states were considered for the 6LU7 and 7JUN structures in order to assess their influence on the structural and dynamical properties in aqueous solution. In the **STD** state, the protonation state for the titratable residues at pH 7 were assigned according to previous Poisson-Boltzmann *pKa* calculations carried for several X-ray structures.[5] All lysines, arginines, aspartic and glutamic acids were modelled in their charged state at pH 7 while all cysteines, histidines and tyrosines were kept neutral. Basing on the pK_a calculations and on the inspection of the nearby contacts, His_{41} and His_{80} were protonated at Nδ whereas His_{64}, His_{163}, His_{164}, His_{172}, and His_{246} were protonated at Nε. The global charge of the protein (dimer form) in the **STD** state amounts to -8 e. The second charge state (**ZW**) corresponds to that characterized in the neutron structure (7JUN) of the SARS-COV-2

enzyme.[2] In this structure, the catalytic dyad adopts a *zwitterionic* state with a negatively charged Cys_{145} thiolate and a doubly protonated His_{41} side chain. According to the 7JUN structure, His_{64}, His_{80}, and His_{164}, are doubly protonated and positively charged, meanwhile His_{163}, His_{172}, and His_{246} are singly protonated and neutral (His_{163} protonated at Nδ1; His_{172} and His_{246} protonated at Nε2). Besides Cys_{145} in the catalytic dyad, residues Cys_{22}, Cys_{38}, Cys_{44}, and Cys_{128} also contain deprotonated thiolates. The global charge of the protein (dimer form) in the **ZW** state amounts to -10 e.

The missing H atoms in the enzyme/peptide complexes were added by the tLEaP program included in the AMBER18 suite of programs.[6] The systems were represented with the ff14SB version[7] of the all-atom AMBER force field and immersed in an octahedral water box that extended 20 Å from the protein atoms. The TIP3P potential[8] was used to represent the water molecules and Na^+ /Cl^- counterions[9] were added with the tLEaP program to neutralize the systems at 0.150 *M* ionic strength.

Molecular dynamics settings

The computational protocol for the molecular dynamics (MD) simulations was analogous to that employed in our previous work.[5] The SHAKE algorithm [10] was selected to constraint all R-H bonds. Periodic boundary conditions were applied together with a non-bonded cutoff of 9.0 Å while long-range interactions were described with the Particle-Mesh-Ewald method.[11] Waters and counterions were first relaxed by means of energy minimizations and 100 *ps* of MD using the SANDER program.[12] After full relaxation, the models were heated gradually from 50 to 300 *K* by carrying out 60 *ps* of constant volume (*NVT*) MD with a 1 *fs* time step and using the PMEMD program in AMBER18. Subsequently, the density was adjusted by means of 2.0 *ns* of constant pressure (*NPT*) MD with a 2 *fs* time step and using the Monte Carlo barostat as implemented in PMEMD. Langevin dynamics was employed to control the temperature (300 *K*) with a collision frequency of 2 ps^{-1}. The production phase of the simulations at the NPT conditions extended up to 2.0 μs and coordinates were saved every 2.5

ps for analysis. The MD runs with a time step of 2.0 *fs* employed the GPU accelerated version of the PMEMD code included in AMBER 18.[12];[13]

Analysis of the MD trajectories

The CPPTRAJ software[14] was used to measure the root mean squared deviation (RMSD) of the protein coordinates with respect to the reference X-ray structures as well as to perform clustering calculations using the average-linkage algorithm (sieve of 250 frames and a RMSD distance metric between frames).

H-bond/vdW contacts and the relative orientation of the protein domains were characterized using software developed locally. H-bonds were identified in terms of heavy atom X···Y distance < 3.5 Å and X-H···Y angle > 120º. To analyze the contacts of the Cys_{145} thiol group, we selected geometric criteria (S_γ···:X distance < 4.0 Å and 90 < S_γH···:X angle < 180º) that take into account the larger size and more diffuse electron cloud of the sulfur atom.[15] Hydrophobic interactions were scored in terms of a dispersion attraction term.[16] The criteria for assessing the occurrence of dispersion interactions were: (a) the total pairwise dispersion energy is larger than 0.5 kcal/mol in absolute value; (b) the distance between the centers of mass of the two interacting groups is below 12.0 Å. The inter-protomer orientation was monitored in terms of the Euler angles (*xyx* convention) between two rigid coordinate systems, which were placed at the center of mass of the protomers. Each coordinate system was defined by the principal inertia axes, which, in turn, were computed considering the coordinates of the backbone atoms located in the α-helical or β-strand elements.

The Chimera visualization system[17] was employed to draw the ribbon/stick models of the systems.

References

1. Z. Jin, X. Du, Y. Xu, Y. Deng, M. Liu, Y. Zhao, B. Zhang, X. Li, L. Zhang, C. Peng, Y. Duan, J. Yu, L. Wang, K. Yang, F. Liu, R. Jiang, X. Yang, T. You, X. Liu, X. Yang, F. Bai, H. Liu, X. Liu, L. W. Guddat, W. Xu, G. Xiao, C. Qin, Z. Shi, H. Jiang, Z. Rao and H. Yang, *Nature*, 2020, **582**, 289-293.
2. D. W. Kneller, G. Phillips, K. L. Weiss, S. Pant, Q. Zhang, H. M. O'Neill, L. Coates and A. Kovalevsky, *J. Biol. Chem.* , 2020, **295**, 17365-17373.
3. X. Xue, H. Yu, H. Yang, F. Xue, Z. Wu, W. Shen, J. Li, Z. Zhou, Y. Ding, Q. Zhao, X. C. Zhang, M. Liao, M. Bartlam and Z. Rao, *J. Virol.*, 2008, **82**, 2515-2527.
4. T. U. Consortium, *Nucleic Acids Res.*, 2019, **47**, D506-D515.
5. D. Suárez and N. Díaz, *J. Chem. Inf. Model*, 2020, **60**, 5815-5831.
6. I. Y. B.-S. D.A. Case, S.R. Brozell, D.S. Cerutti, T.E. Cheatham, III, V.W.D. Cruzeiro, T.A. Darden, R.E. Duke, D. Ghoreishi, M.K. Gilson, H. Gohlke, A.W. Goetz, D. Greene, R Harris, N. Homeyer, S. Izadi, A. Kovalenko, T. Kurtzman, T.S. Lee, S. LeGrand, P. Li, C. Lin, J. Liu, T. Luchko, R. Luo, D.J. Mermelstein, K.M. Merz, Y. Miao, G. Monard, C. Nguyen, H. Nguyen, I. Omelyan, A. Onufriev, F. Pan, R. Qi, D.R. Roe, A. Roitberg, C. Sagui, S. Schott-Verdugo, J. Shen, C.L. Simmerling, J. Smith, R. Salomon-Ferrer, J. Swails, R.C. Walker, J. Wang, H. Wei, R.M. Wolf, X. Wu, L. Xiao, D.M. York, P.A. Kollman, University of California, San Francisco, 2018.
7. J. A. Maier, C. Martinez, K. Kasavajhala, L. Wickstrom, K. E. Hauser and C. Simmerling, *J. Chem. Theory Comput.*, 2015, **11**, 3696-3713.
8. W. L. Jorgensen, J. Chandrasekhar, J. D. Madura, R. W. Impey and M. L. Klein, *J. Chem. Phys.*, 1983, **79**, 926-935.
9. I. S. Joung and T. E. Cheatham, *J. Phys.Chem. B*, 2009, **113**, 13279-13290.
10. J.-P. Ryckaert, G. Ciccotti and H. J. C. Berendsen, *J. Comput. Phys.*, 1977, **23**, 327-341.
11. U. Essmann, L. Perera, M. L. Berkowitz, T. Darden, H. Lee and L. G. Pedersen, *J. Chem. Phys.*, 1995, **103**, 8577–8593.
12. R. Salomon-Ferrer, D. A. Case and R. C. Walker, *WIREs Comput Mol Sci*, 2013, **3**, 198-210.
13. S. Le Grand, A. W. Götz and R. C. Walker, *Comput. Phys. Commun.*, 2013, **184**, 374-380.
14. D. R. Roe and T. E. Cheatham, *J. Chem. Theory Comput.*, 2013, **9**, 3084-3095.
15. P. Zhou, F. Tian, F. Lv and Z. Shang, *Proteins*, 2009, **76**, 151-163.
16. M. Elstner, P. Hobza, T. Frauenheim, S. Suhai and E. Kaxiras, *J. Chem. Phys.*, 2001, **114**, 5149-5155.
17. E. F. Pettersen, T. D. Goddard, C. C. Huang, G. S. Couch, D. M. Greenblatt, E. C. Meng and T. E. Ferrin, *J Comput Chem.*, 2004, **25**, 1605-1612.

Figure S1. Time evolution along the different trajectories of the root mean squared deviation (RMSD) computed for selected backbone heavy atoms (in Å) with respect to the initial structure (6LU7 or 7JUN). The plots in red correspond to the protonation state provided by the neutron diffraction experiments (**ZW**) and the plots in blue are for the standard (**STD**) protonation state.

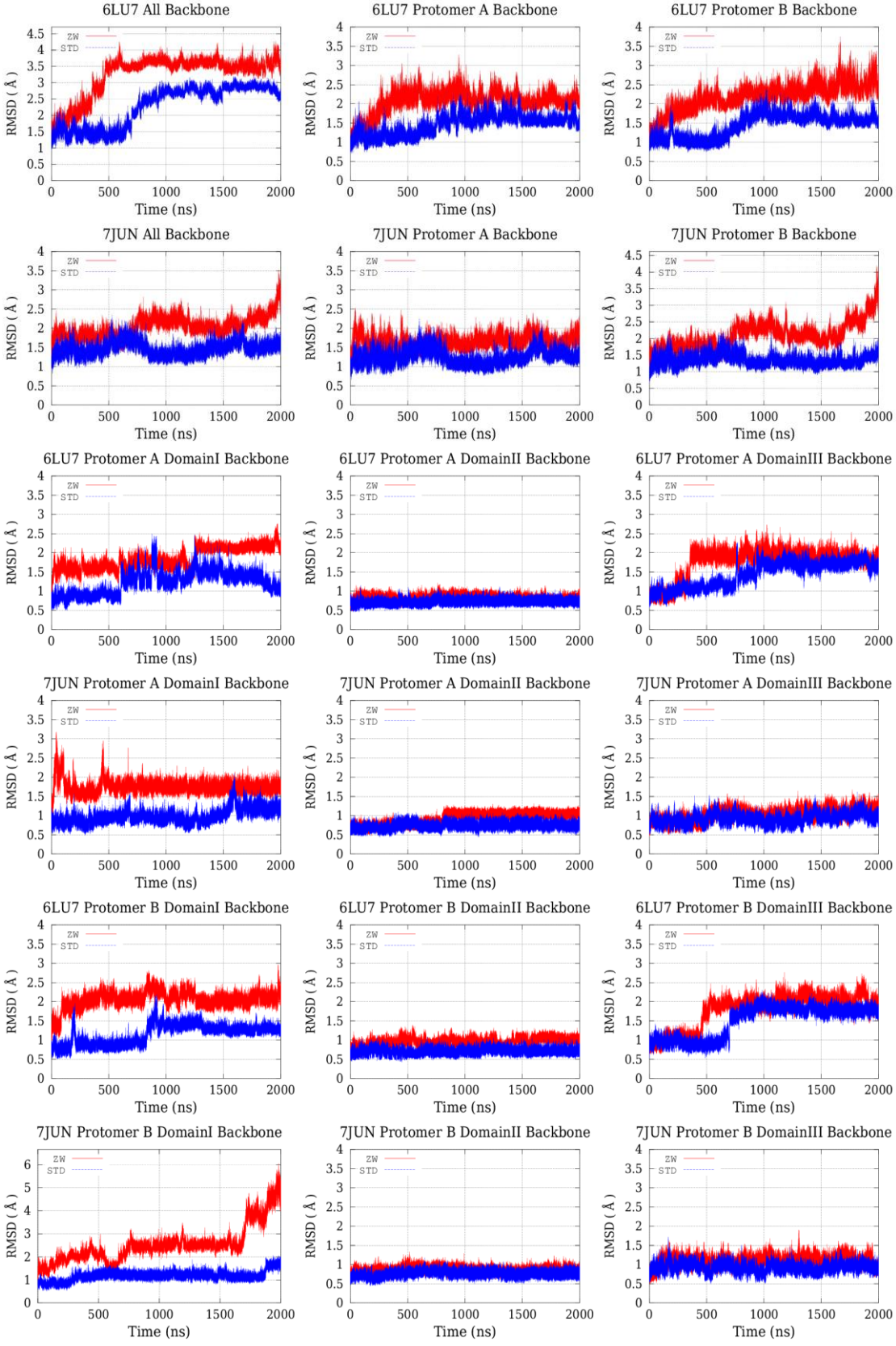

Figure S2. Dial plots of the Euler rotational angles, ϕ (red) θ (blue) and ψ (green) (*xyx* convention), of the protomer A with respect to protomer B. The radius is the time axis (0-2000 ns).

6LU7_STD

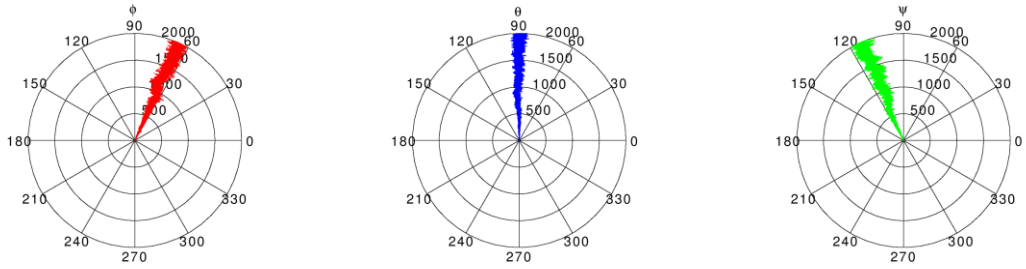

6LU7_ZW

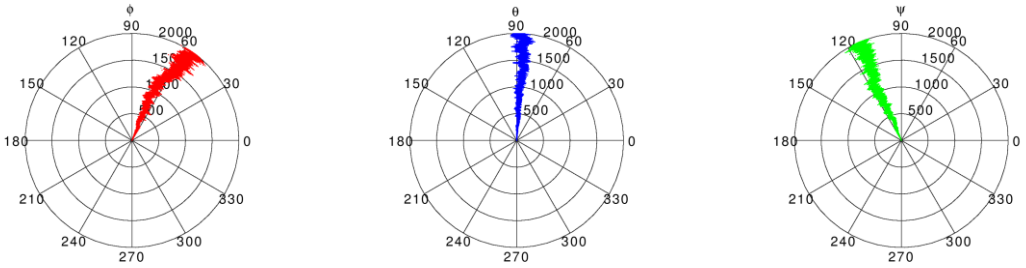

7JUN_STD

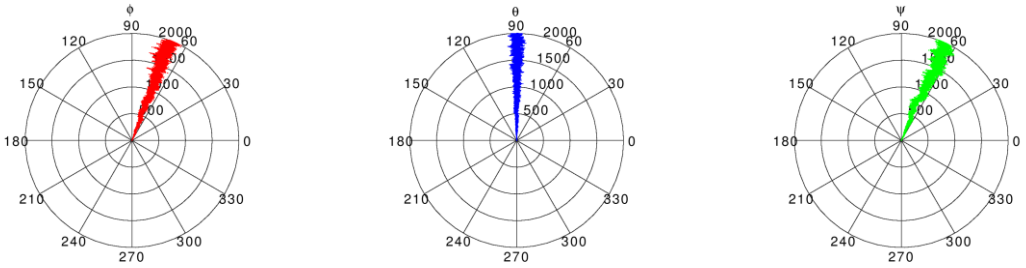

7JUN_ZW

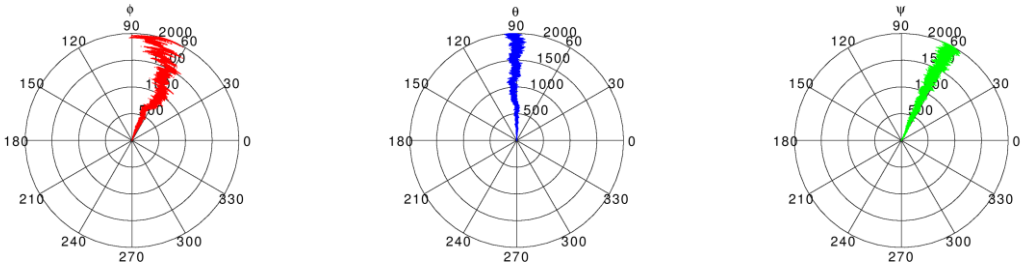

Figure S3 Different views for a ribbon representation of the average structure obtained from the last 50 ns of the MD simulations. The average structures were superposed over the 6LU7/7JUN structures (in lighter color) using the backbone coordinates of the domain II.

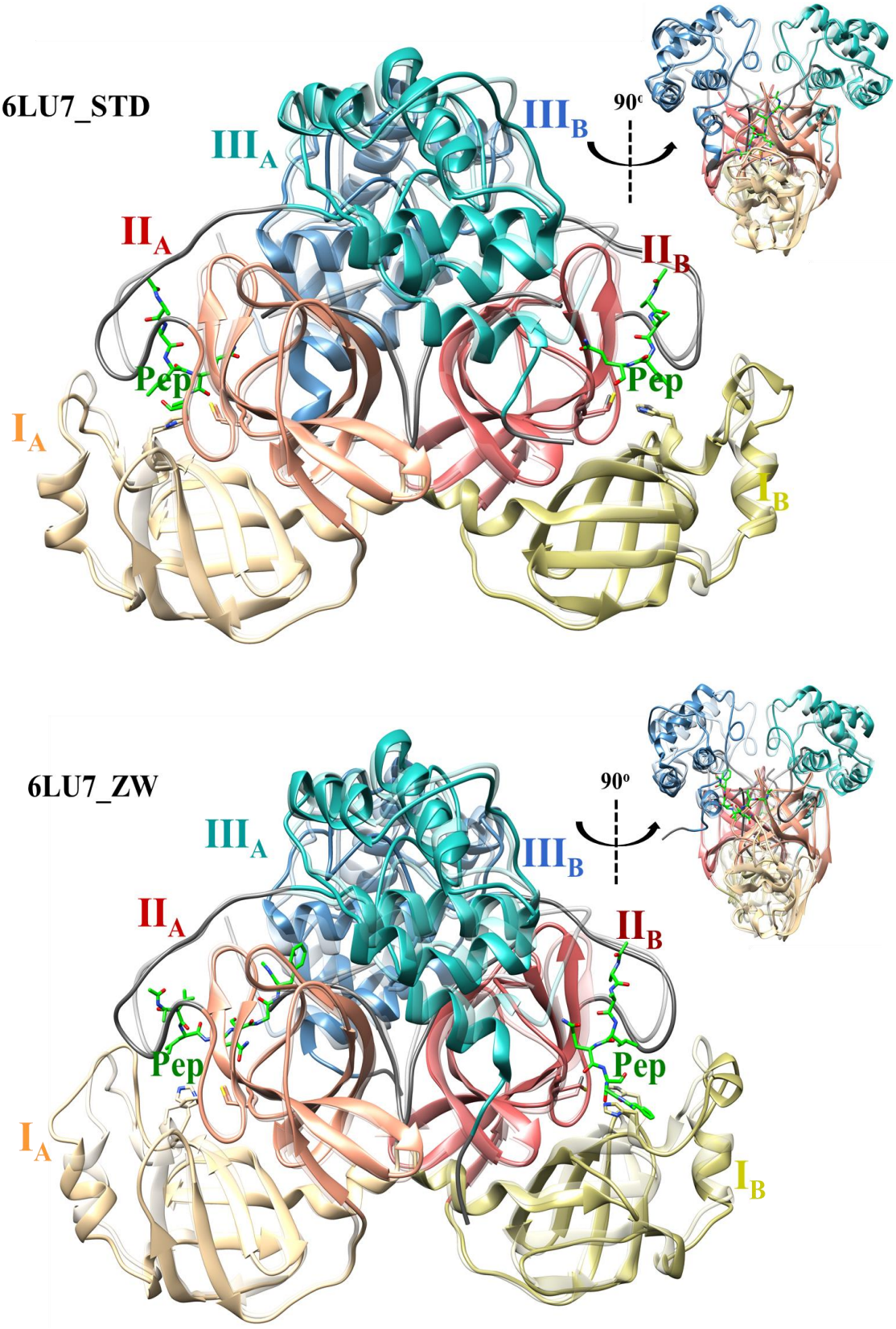

Figure S3 (cont.)

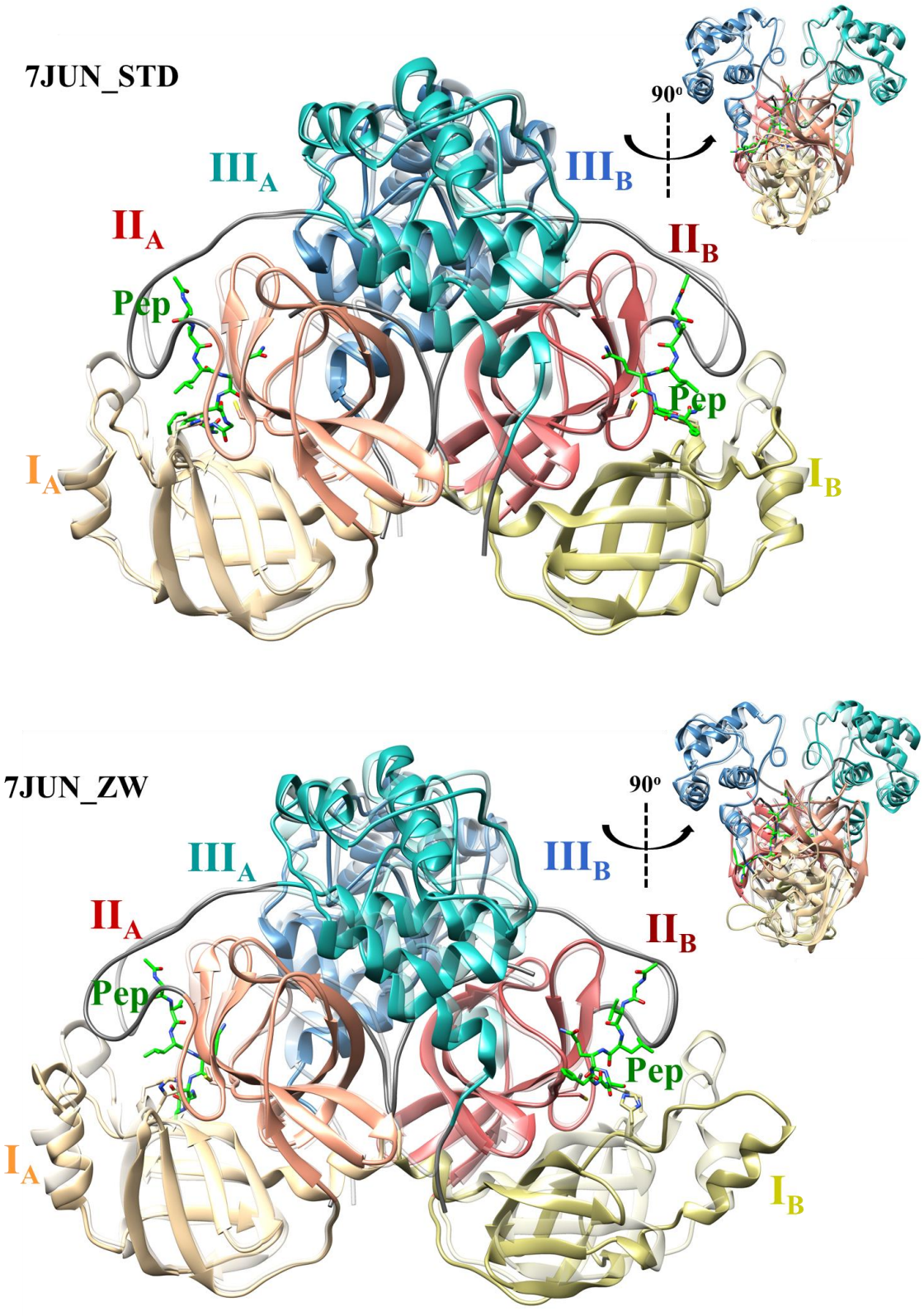

Table S1. Most abundant **polar contacts between the A and B protomers**[(a)] characterized along the last 1.5 μs of the different MD simulations. Percentage of abundance (%), and average distances between heavy atoms (*d*) in Å are provided.

	6LU7_STD		**6LU7_ZW**		**7JUN_STD**		**7JUN_ZW**	
A···B	*%*	*d*	*%*	*d*	*%*	*d*	*%*	*d*
Ser_{1}@O···Phe_{140}@NH	95	3.08	--	--	75	3.05	--	--
Phe_{140}@NH···Ser_{1}@O	96	3.09	73	3.14	87	3.07	--	--
Ser_{1}@Oγ···His_{172}@Nε2H	77	3.06	--	--	70	3.09	--	--
His_{172}@Nε2H···Ser_{1}@Oγ	75	3.07	--	--	74	3.06	--	--
Ser_{1}@O···His_{172}@Nε2H	59	3.22	--	--	57	3.21	--	--
His_{172}@Nε2H···Ser_{1}@O	58	3.23	57	3.21	53	3.32	--	--
Arg_{4}@NηH···Glu_{290}@Oε	86	2.97	29	2.97	74	2.98	--	--
Glu_{290}@Oε···Arg_{4}@NηH	85	2.95	41	2.95	99	2.78	--	--
Arg_{4}@NεH···Lys_{137}@O	89	2.87	--	--	77	2.87	--	--
Lys_{137}@O···Arg_{4}@NεH	87	2.86	--	--	99	2.88	--	--
Arg_{4}@NηH···Lys_{137}@O	85	2.93	42	2.87	75	2.94	100	2.84
Lys_{137}@O···Arg_{4}@NηH	84	2.92	85	2.85	98	2.92	82	2.85
Arg_{4}@NηH···Cys_{128}@Sγ	51	3.5	51	3.2	52	3.5	98	3.3
Cys_{128}@Sγ···Arg_{4}@ NηH	47	3.5	96	3.2	49	3.5	97	3.3
Ala_{7}@O···Val_{125}@NH	**100**	**2.93**	**91**	**3.14**	**99**	**2.96**	**99**	**2.99**
Val_{125}@NH···Ala_{7}@O	**100**	**2.94**	**100**	**2.93**	**99**	**3.00**	**99**	**3.00**
Ala_{7}@NH···Val_{125}@O	**99**	**2.99**	**81**	**3.14**	**98**	**3.02**	**100**	**2.96**
Val_{125}@O···Ala_{7}@NH	**99**	**3.00**	**98**	**2.99**	**99**	**3.00**	**87**	**3.15**
Pro_{9}@O···Glu_{14}@Oε (Wat)	79	4.38	77	4.51	62	4.35	65	4.36
Glu_{14}@Oε···Pro_{9}@O (Wat)	96	4.40	82	4.43	90	4.39	78	4.49
Ser_{10}@Oγ···Ser_{10}@NH	97	3.06	98	3.06	95	3.07	96	3.05
Ser_{10}@NH···Ser_{10}@Oγ	98	3.06	96	3.06	97	3.05	96	3.07

[a] Data in bold correspond to highly persistent contacts.

Table S1 (cont.).

	6LU7_STD		**6LU7_ZW**		**7JUN_STD**		**7JUN_ZW**	
A···B	*%*	*d*	*%*	*d*	*%*	*d*	*%*	*d*
Gly_{11}@NH···Glu_{14}@Oε	91	2.92	100	2.91	83	2.99	80	2.98
Glu_{14}@Oε···Gly_{11}@NH	100	2.87	100	2.87	100	2.90	100	2.91
Lys_{12}@NH···Glu_{14}@Oε (Wat)	78	4.38	82	4.45	62	4.41	64	4.42
Glu_{14}@Oε ···Lys_{12}@NH (Wat)	93	4.35	92	4.30	91	4.39	85	4.38
Ser_{123}@O···Arg_{298}@Nε/NηH	46	2.89	52	2.94	20	5.01	87	5.12
Arg_{298}@ Nε/NηH···Ser_{123}@O	31	5.38	77	5.62	19	2.91	46	5.62
Ser_{139}@OγH···Gln_{299}@Oε/Nε	62	2.73	61	2.72	74	2.71	36	4.34
Gln_{299}@Oε/NεH···Ser_{139}@OγH	85	2.74	71	2.93	82	2.78	96	2.75
Pro_{122}@O···Phe_{305}@NH	--	--	--	--	97	2.94	98	2.92

Table S2. Most abundant **hydrophobic contacts between the A and B protomers**[(a)] characterized along the last 1.5 μs of the different MD simulations. Percentage of abundance (%), average distances between side chains (*d*) in Å, and interaction energies (*E*) in kcal/mol are provided.

	6LU7_STD			**6LU7_ZW**			**7JUN_STD**			**7JUN_ZW**		
A···B	*%*	*d*	*E*	*%*	*d*	*E*	*%*	*d*	*E*	*%*	*d*	*E*
Met_6···Tyr_{126}	**100**	**5.60**	**-1.31**	**100**	**6.08**	**-0.93**	**100**	**5.38**	**-1.51**	**100**	**5.46**	**-1.49**
Tyr_{126}···Met_6	**100**	**5.63**	**-1.29**	**100**	**5.52**	**-1.46**	**100**	**5.53**	**-1.37**	**100**	**5.62**	**-1.28**
Pro_9···Pro_{122}	100	5.71	-0.79	100	5.61	-0.85	100	5.58	-0.87	100	5.55	-0.89
Pro_{122}···Pro_9	100	5.74	-0.77	100	5.70	-0.81	100	5.44	-0.97	100	5.71	-0.79
Pro_9···Val_{125}	100	5.62	-0.63	100	6.05	-0.48	100	5.69	-0.61	100	6.08	-0.44
Val_{125}···Pro_9	100	5.57	-0.64	100	5.38	-0.75	100	6.01	-0.47	100	5.78	-0.55
Pro_9···Leu_{115}	100	6.11	-0.70	100	6.41	-0.55	100	6.19	-0.65	100	6.29	-0.59
Leu_{115}···Pro_9	100	6.06	-0.72	100	5.98	-0.77	100	6.29	-0.59	100	6.38	-0.57
Val_{125}···Val_{125}	**100**	**5.25**	**-0.81**	**100**	**5.06**	**-0.90**	**100**	**5.30**	**-0.79**	**100**	**5.30**	**-0.80**
Ala_{285}···Leu_{286}	99	4.60	-0.60	79	4.98	-0.50	99	4.58	-0.61	100	4.37	-0.68
Leu_{286}···Ala_{285}	99	4.56	-0.62	77	4.96	-0.50	94	4.60	-0.61	99	4.36	-0.68

[(a)] Data in bold correspond to strong and conserved contacts.

Figure S4. Time evolution along the different trajectories of the RMSD computed for the *N*-finger and the Arg_{40}-Pro_{52} backbone heavy atoms (in Å) with respect to the initial structure (6LU7 or 7JUN). The plots in red correspond to the protonation state provided by the neutron diffraction experiments (**ZW**) and the plots in blue are for the standard (**STD**) protonation state.

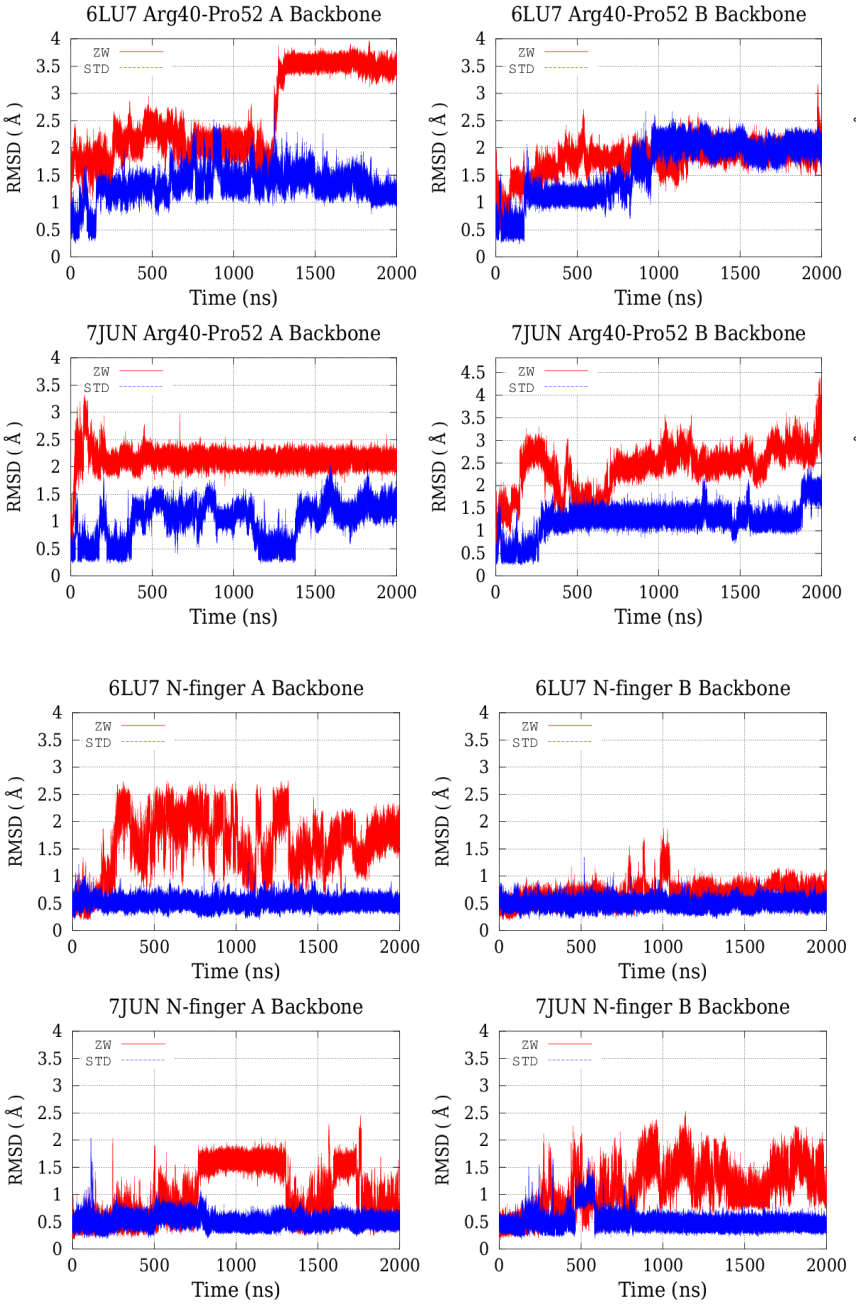

Table S3. Average values and standard deviation of the RMSD data (in Å; last 1.5 μs) computed for the secondary structural elements in protomers A/B including Cys/His residues with different charge state in the **STD** and **ZW** configurations.[(a)]

Residues	Structural Element	**6LU7_STD**	**6LU7_ZW**	**7JUN_STD**	**7JUN_ZW**
Cys_{22}	β sheet $strand_{17-22}$	0.5±0.2/0.5±0.2	0.5±0.1/**0.9±0.1**	0.5±0.2/0.7±0.1	0.6±0.1/0.6±0.2
Cys_{38}	β sheet $strand_{35-39}$	0.3±0.1/0.3±0.1	**0.7±0.1/0.7±0.1**	0.3±0.1/0.3±0.1	**0.6±0.1/0.6±0.2**
His_{41}, Cys_{44}	$Helix_{41-44}$	0.3±0.1/0.3±0.1	**0.8±0.2/1.3±0.2**	0.3±0.1/0.5±0.1	**1.8±0.1/1.6±0.1**
Cys_{128}	β sheet $strand_{121-129}$	0.4±0.1/0.4±0.1	0.6±0.1/0.6±0.1	0.4±0.1/0.4±0.1	0.4±0.1/0.4±0.1
Cys_{145}	$Loop_{130-147}$	0.5±0.1/0.5±0.1	0.6±0.1/0.8±0.1	0.5±0.1/0.6±0.1	**1.0±0.1**/0.7±0.1
His_{64}	$Helix_{62-66}$	0.3±0.1/0.4±0.1	0.4±0.1/0.4±0.1	0.4±0.1/0.4±0.1	0.5±0.1/0.5±0.1
His_{80}	β sheet $strand_{77-83}$	1.0±0.2/0.6±0.1	1.0±0.2/0.7±0.2	0.5±0.1/0.5±0.1	0.5±0.1/**1.5±0.4**
His_{164}	β sheet $strand_{157-166}$	0.4±0.1/0.4±0.1	0.4±0.1/0.4±0.1	0.4±0.1/0.4±0.1	0.4±0.1/0.4±0.1

[(a)] RMSD data in bold correspond to structural elements with larger deviations in the **ZW** configurations than in the **STD** ones.

Table S4. Details of the average-linkage clustering calculations (last 1.5 μs) with best-fit coordinate RMSD metric and a threshold value of 1.5 Å including coordinates of either backbone or conformationally-unique side-chain heavy atoms for a selection of residues around the catalytic dyad comprising a total of 447 (backbone + side chain) atoms.

Trajectory	**# of clusters**	**% Abundance of the top 4 clusters**			
		backbone + side chain			
7JUN-ZW$_A$	5	71.1	22.5	4.0	2.1
7JUN-ZW$_B$	105	12.0	8.4	7.3	5.2
7JUN-STD$_A$	2	66.5	33.5		
7JUN-STD$_B$	2	98.5	1.5		
6LU7-ZW$_A$	10	36.6	28.6	13.0	9.1
6LU7-ZW$_B$	10	46.8	17.5	7.5	1.5
6LU7-STD$_A$	14	40.5	26.5	10.0	8.3
6LU7-STD$_B$	10	49.0	22.0	16.9	4.6

Figure S5. View of the active site as shown by the superposition of the most important cluster representatives (coil thickness and color intensity are proportional to cluster abundance).

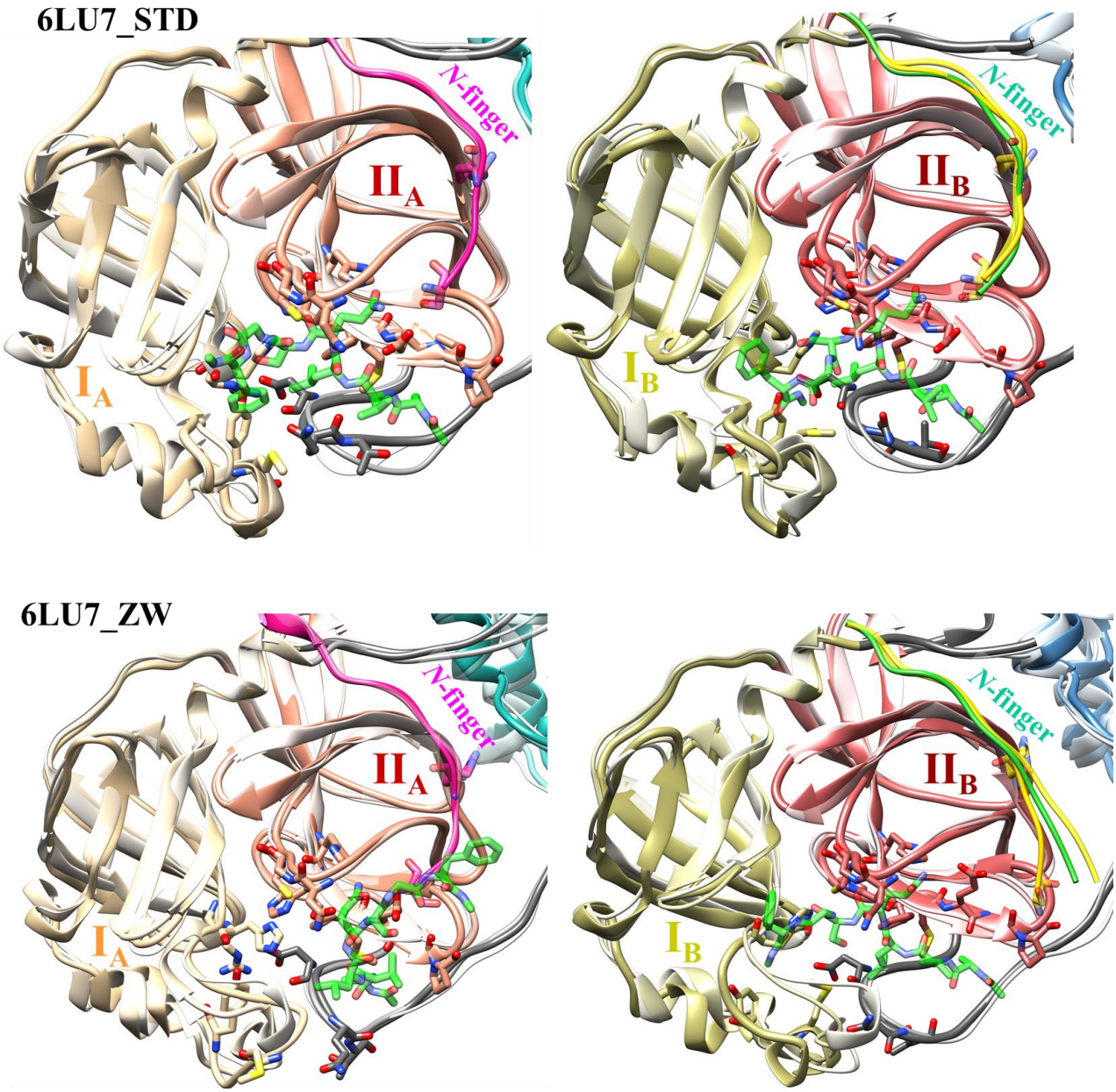

Figure S7 (cont.)

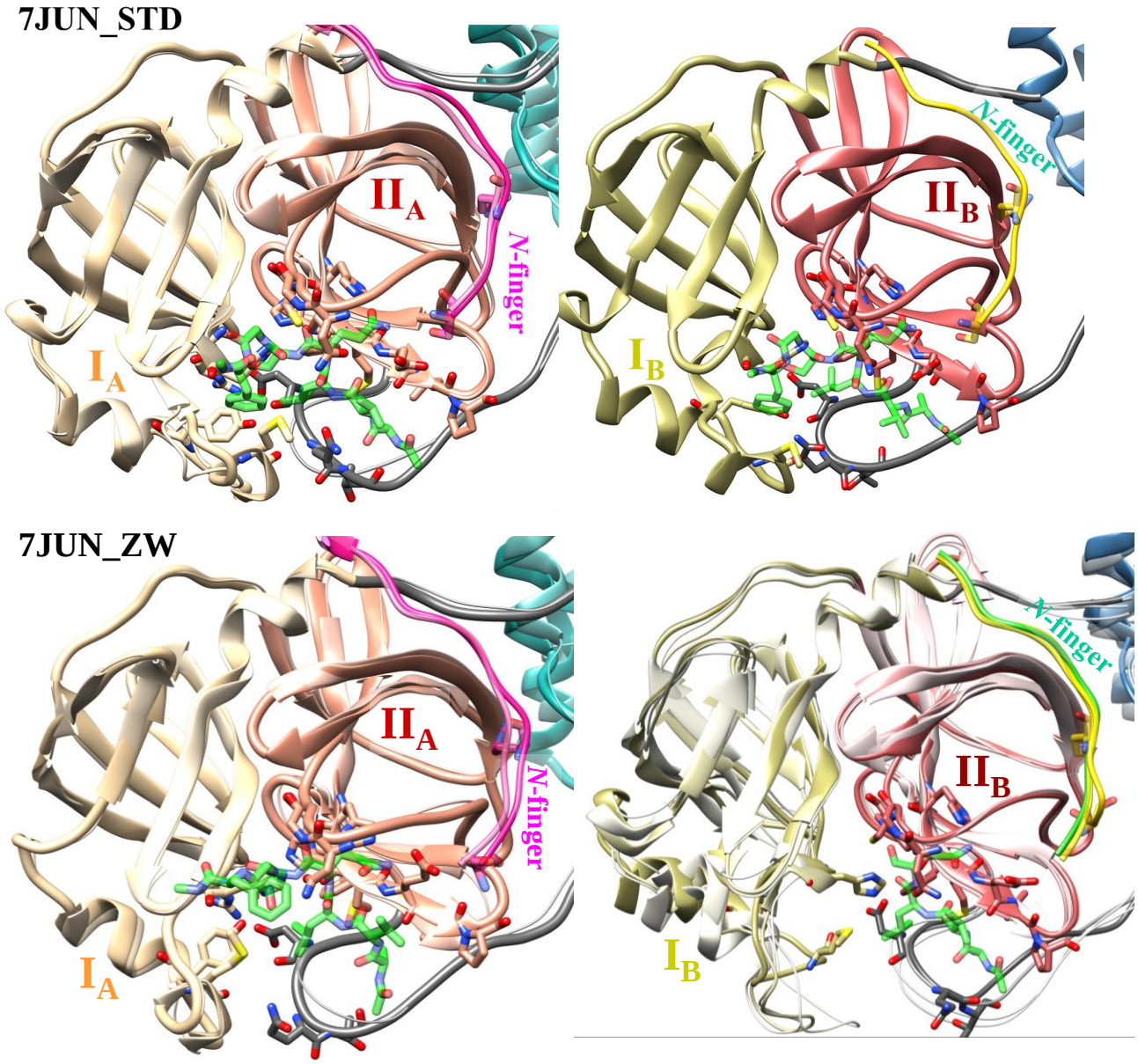

Figure S6. a) Views of the active site region (protomers A/B) showing the peptide substrate and the catalytic residues in the most populated cluster representative. The backbone atoms of the scissile peptide bond are displayed in ball-and-stick. **b)** Histogram representation of the values computed for the relevant distance (in Å) between the Cys_{145}@Sγ nucleophile and Gln(P_1)@C at the scissile peptide bond. **c)** Schematic representations of the enzyme-substrate and catalytic-dyad interactions. Average values of heavy-atom separation (Å) and % of abundances are indicated for selected contacts. For the **STD** models, only one scheme is represented with some abundances segregated into protomer A/protomer B values.

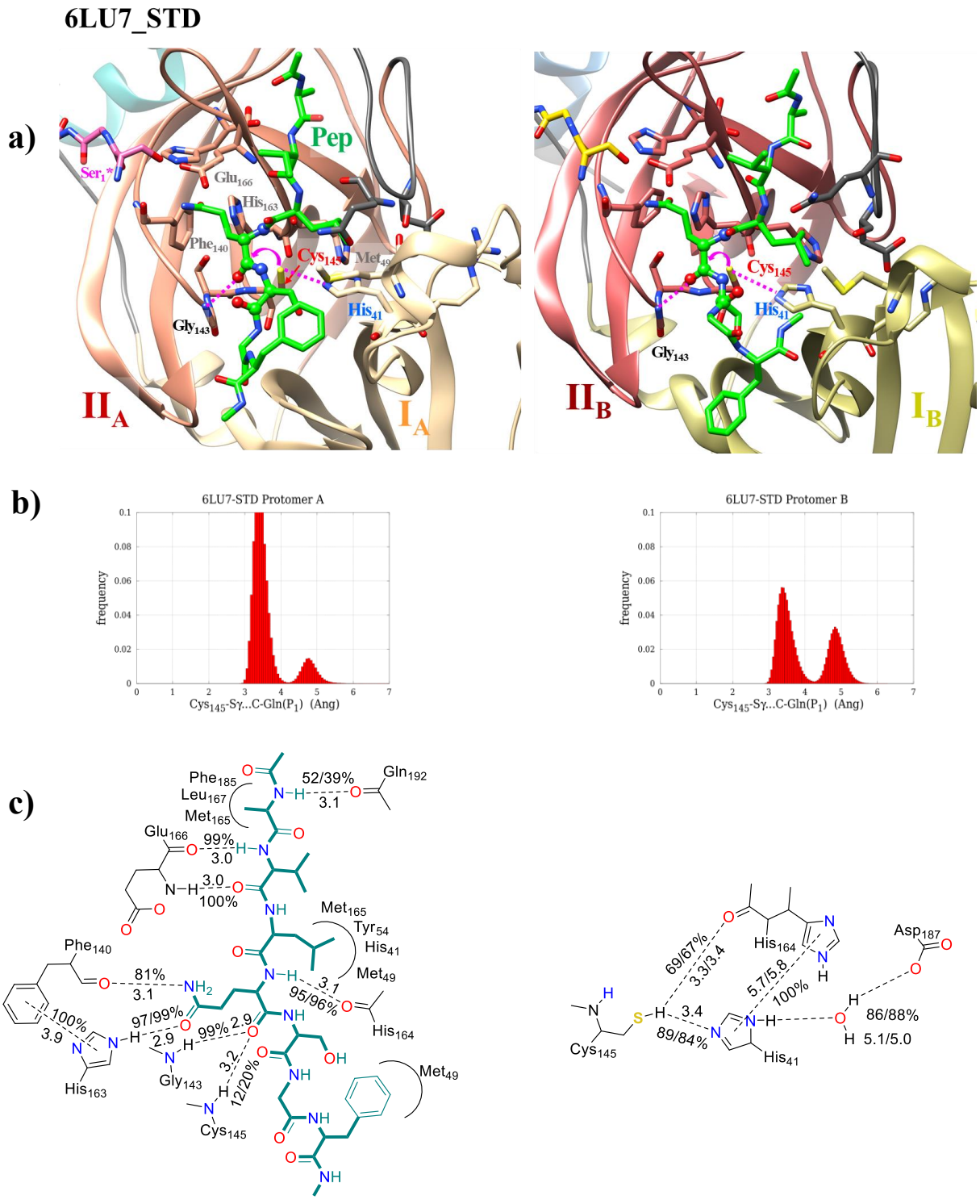

Figure S6 (cont.)

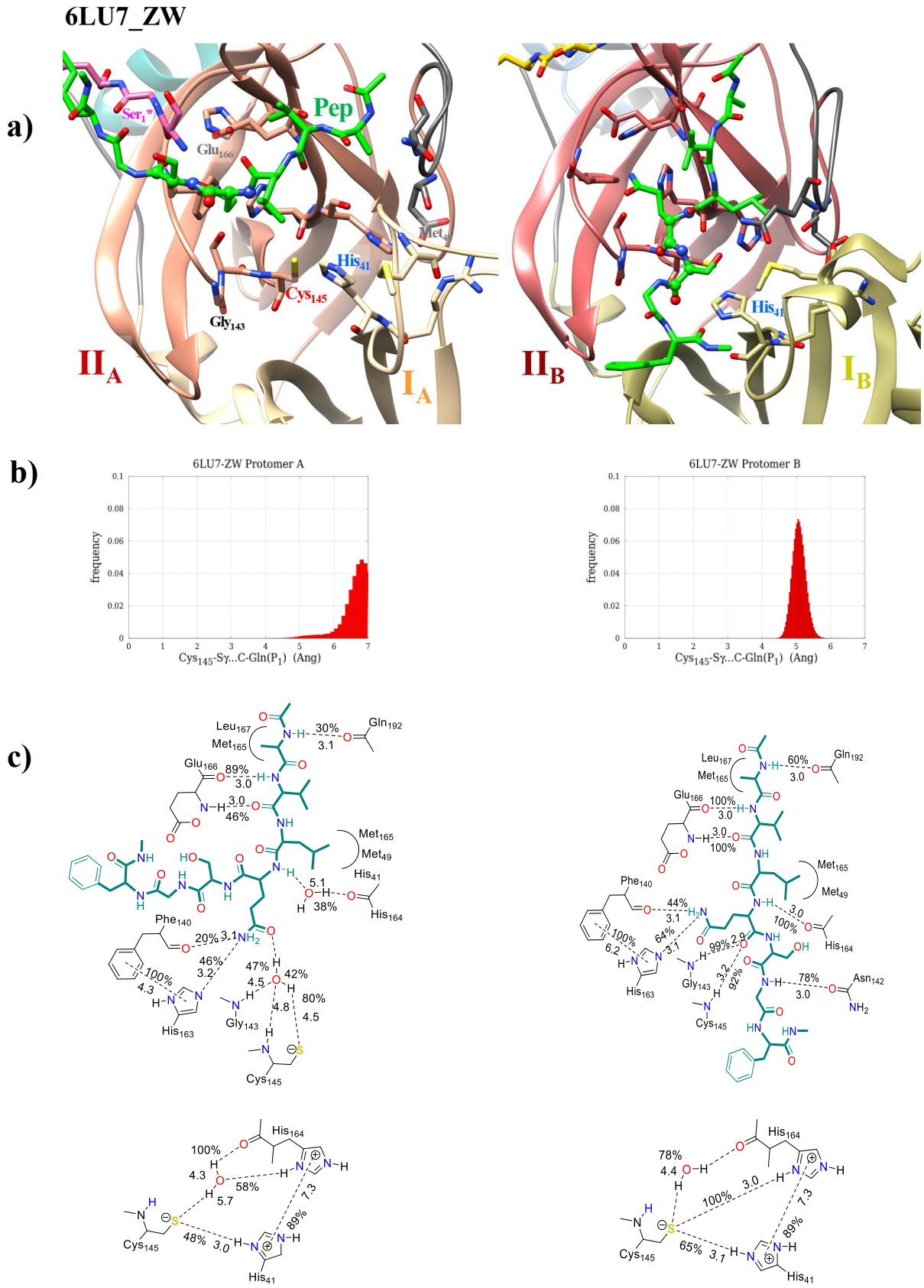

Figure S6 (cont.)

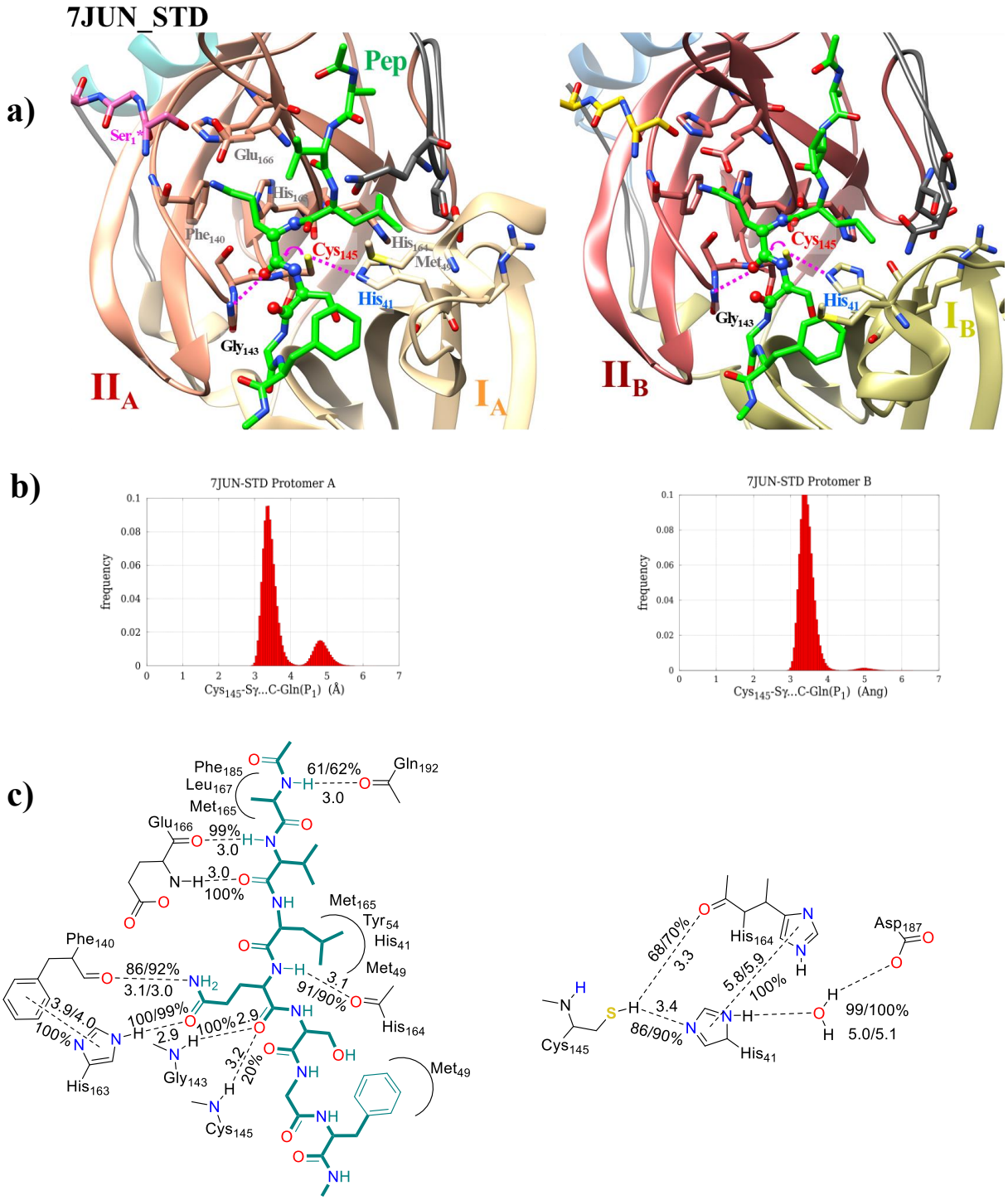

Figure S6 (cont.)

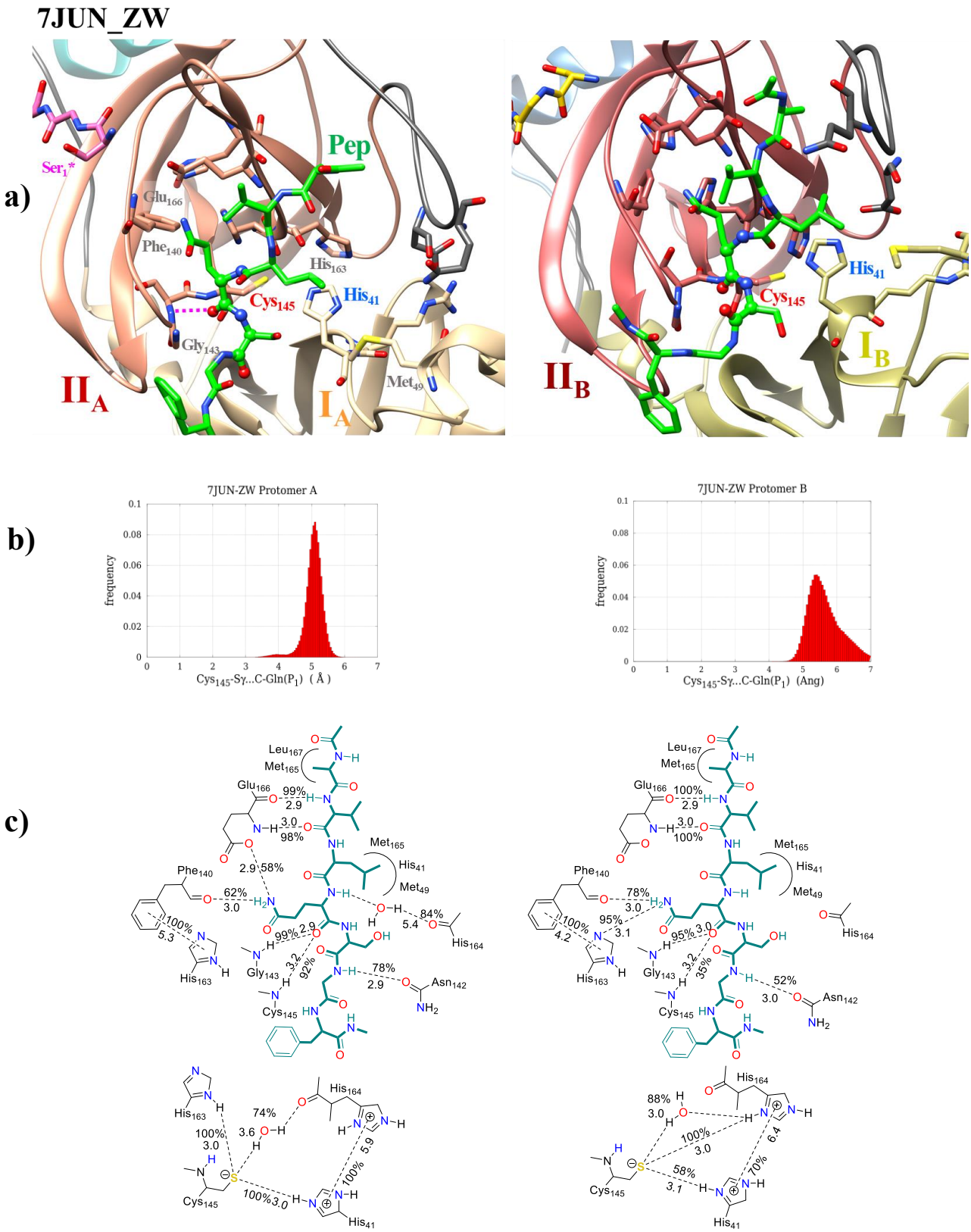

Table S5. Most abundant **polar contacts between active site residues** characterized along the last 1.5 μs of the different MD simulations. Percentage of abundance (%) and average distances between heavy atoms (*d*, in Å) are provided for protomers A and B.

	6LU7_STD				6LU7_ZW				7JUN_STD				7JUN_ZW			
Contacts	$\%_A$	$\%_B$	d_A	d_B	$\%_A$	$\%_B$	d_A	d_B	$\%_A$	$\%_B$	d_A	d_B	$\%_A$	$\%_B$	d_A	d_B
His_{41}@O···Cys_{44}@NH	81	89	3.2	3.1	18	--	3.4	--	78	62	3.2	3.3	--	--	--	--
His_{41}@NH···Asp_{187}@Oδ (Wat)	77	78	4.4	4.4	--	--	--	--	67	41	4.6	5.0	--	--	--	--
His_{41}@Nδ1H···Asp_{187}@Oδ (Wat)	**86**	**88**	**5.1**	**5.0**	**--**	**--**	**--**	**--**	**99**	**100**	**5.0**	**5.1**	**26**	**--**	**5.1**	**--**
His_{41}@Nδ1H···Cys_{85}@O (Wat)	82	67	5.4	5.5	--	--	--	--	51	36	5.6	5.6	--	--	--	--
His_{41}@Nε2···Cys_{145}@Sγ	**89**	**84**	**3.4**	**3.4**	**17[(b)]**	**65**	**3.0**	**3.1**	**86**	**90**	**3.4**	**3.4**	**100**	**22[(b)]**	**3.0**	**3.7**
His_{41}@Nδ1H···Cys_{145}@Sγ	--	--	--	--	48	27[(b)]	3.0	4.2	--	--	--	--	--	58	--	3.1
His_{41}@Nδ1H···His_{164}@Nδ (Wat)	35	32	4.0	4.0	7[(b)]	--	5.8	--	53	55	4.1	4.0	--	--	--	--
His_{41}@Nε2H···His_{164}@O	--	--	--	--	50[(b)]	--	5.4	--	--	--	--	--	71	12[(b)]	3.2	5.3
His_{41}@NH···Cys_{38}@Sγ (Wat)	--	--	--	--	--	67	--	4.5	--	--	--	--	98	73	4.8	5.2
His_{41}@O···Ile_{43}@NH	6	--	3.3	--	10	--	3.1	--	6	11	3.1	3.1	98	6	2.9	3.2
His_{41}@Nδ1H···Tyr_{54}@Oη (Wat)	--	6	--	4.8	--	--	--	--	--	--	--	--	89	7	5.4	5.1
Cys_{145}@O···Asn_{28}@Nδ2H	99	98	3.0	3.0	98	100	2.9	2.9	98	97	3.0	3.0	99	99	2.9	2.9
Cys_{145}@O···Asn_{28}@NH	85	74	3.2	3.2	47	66[(b)]	3.3	4.7	91	91	3.2	3.2	92	51	3.2	3.3
Cys_{145}@Sγ···His_{164}@O	**69**	**67**	**3.3**	**3.4**	**100[(b)]**	**78[(b)]**	**4.3**	**4.4**	**68**	**70**	**3.3**	**3.3**	**74[(b)]**	**35[(b)]**	**3.6**	**4.3**
Cys_{145}@Sγ···His_{164}@Nδ1H	**--**	**--**	**--**	**--**	**58[(b)]**	**100**	**5.7**	**3.0**	**--**	**--**	**--**	**--**	**--**	**100**	**--**	**3.0**
Cys_{145}@Sγ···His_{163}@Nδ1H	--	--	--	--	40	--	3.3	--	--	--	--	--	100	--	3.0	--

[(a)] Data in bold correspond to important contacts that are highly persistent in the **STD** models, but are weakened or lost in the **ZW** ones.

[(b)] Water-mediated contact.

Table S5 (cont.)

	6LU7_STD				6LU7_ZW				7JUN_STD				7JUN_ZW			
Contacts	$\%_A$	$\%_B$	d_A	d_B	$\%_A$	$\%_B$	d_A	d_B	$\%_A$	$\%_B$	d_A	d_B	$\%_A$	$\%_B$	d_A	d_B
His_{163}@NH···Ser_{147}@O	100	100	2.9	2.9	100	100	2.9	2.9	100	100	2.9	2.9	100	100	3.0	2.0
His_{163}@O···Gly_{146}@NH	100	100	3.0	3.0	81	100	3.1	3.0	100	100	3.0	3.0	30	100	3.3	2.9
His_{163}@O···His_{164}@Nδ1H	--	--	--	--	11	--	2.9	--	--	--	--	--	92	--	2.9	--
His_{163}@Nδ1···His_{164}@NH	77	75	3.2	3.2	--	--	--	--	76	70	3.2	3.2	--	--	--	--
His_{163}@Nδ1···Tyr_{161}@OηH	51	60	3.2	3.2	--	42	--	3.3	66	57[(b)]	3.2	4.4	--	29	--	3.2
His_{163}@Nε2H···Ser_{144}@Oγ	78	75	3.2	3.2	--	8	--	2.9	77	91	3.2	3.1	--	--	--	--
His_{164}@Nε2H···Thr_{175}@Oγ	99	99	3.0	3.0	24	100	3.0	2.9	99	99	3.0	3.0	--	88	--	3.0
His_{164}@NH···Ala_{173}@O	83	81	3.2	3.2	69	96	3.1	3.1	83	86	3.2	3.2	100	98	2.9	3.1
His_{164}@Nε2H···Cys_{85}@O	--	--	--	--	74	--	2.8	--	--	--	--	--	100	--	2.8	--
His_{164}@Nδ1H···Met_{162}@O	--	--	--	--	18	--	2.9	--	--	--	--	--	97	--	3.0	--
His_{172}@NH···Ile_{136}@O	100	100	2.9	2.9	98	100	3.0	2.8	100	100	2.9	2.9	100	99	2.9	3.0
His_{172}@O···Ile_{136}@NH	100	100	3.0	3.0	99	98	3.0	3.1	100	100	2.9	2.9	96	96	3.1	3.0
His_{172}@Nε2H···Glu_{166}@Oε	11	9	2.9	2.9	39	30	2.8	2.9	14	18	2.9	2.8	53	42	2.9	2.9
His_{172}@Nδ1···Gly_{138}@NH	72	74	3.3	3.2	58	--	3.3	--	77	68	3.2	3.3	14	53	3.2	3.3

Table S6. Most abundant **hydrophobic contacts between active site residues** characterized along the last 1.5 μs of the different MD simulations. Percentage of abundance (%), average distances between side chains (*d*) in Å, and interaction energies (*E*) in kcal/mol are provided. Subscripts A and B indicates protomers A and B, respectively.

	6LU7_STD						**6LU7_ZW**						**7JUN_STD**						**7JUN_ZW**					
Contacts	$\%_A$	$\%_B$	d_A	d_B	E_A	E_B	$\%_A$	$\%_B$	d_A	d_B	E_A	E_B	$\%_A$	$\%_B$	d_A	d_B	E_A	E_B	$\%_A$	$\%_B$	d_A	d_B	E_A	E_B
$His_{41}\cdots Leu_{27}$	100	100	5.3	5.3	-1.1	-1.2	100	81	5.5	6.1	-1.1	-0.8	100	100	5.3	5.2	-1.1	-1.2	100	91	5.8	7.0	-0.9	-0.3
$His_{41}\cdots Pro_{39}$	100	100	4.9	4.9	-1.2	-1.3	83	100	6.6	5.2	-0.4	-1.0	100	100	5.0	4.8	-1.2	-1.3	100	64	4.5	7.2	-1.6	-0.2
$His_{41}\cdots His_{164}$	100	100	5.7	5.8	-0.8	-0.7	94	89	7.1	7.3	-0.2	-0.2	100	100	5.8	5.9	-0.7	-0.7	100	70	5.9	6.4	-0.6	-0.4
$Phe_{140}\cdots His_{163}$ (a)	100	100	**3.9**	**3.9**	**-3.3**	**-3.3**	100	100	**4.3**	**6.2**	**-2.4**	**-1.6**	100	100	**3.9**	**4.0**	**-3.2**	**-2.9**	100	100	**5.3**	**4.2**	**-1.5**	**-2.6**
$Phe_{140}\cdots Tyr_{126}$	100	100	5.6	5.6	-1.4	-1.4	100	97	5.9	6.3	-1.2	-1.1	100	100	5.9	6.1	-1.2	-1.1	100	100	6.6	5.9	-0.9	-1.3
$Phe_{140}\cdots His_{172}$ (a)	100	100	**5.4**	**5.4**	**-1.2**	**-1.3**	100	100	**5.2**	**4.8**	**-1.5**	**-1.8**	100	100	**5.3**	**5.4**	**-1.3**	**-1.3**	100	100	**4.4**	**5.4**	**-2.4**	**-1.3**
$Phe_{140}\cdots Val_{114}$	100	100	5.9	5.9	-0.9	-0.9	100	100	6.2	6.2	-0.8	-0.8	100	100	6.0	6.0	-0.8	-0.8	99	100	6.9	5.6	-0.5	-1.1
$Phe_{140}\cdots Tyr_{118}$	100	100	7.0	7.1	-0.5	-0.5	91	100	7.2	6.7	-0.4	-0.5	100	100	7.2	7.0	-0.4	-0.5	--	99	--	7.7	--	-0.3
$Phe_{140}\cdots Ala_{116}$	100	100	5.2	5.2	-0.5	-0.5	100	100	5.3	4.3	-0.5	-0.8	100	99	5.2	5.1	-0.5	-0.5	95	99	5.2	5.3	-0.5	-0.5
$Phe_{140}\cdots Met_6$*	--	--	--	--	--	--	--	100	--	6.1	--	-0.8	28	36	8.0	8.0	-0.1	-0.1	72	54	7.9	8.0	-0.2	-0.2
$His_{163}\cdots His_{172}$	100	100	5.6	5.6	-0.8	-0.8	100	100	5.6	4.4	-0.8	-1.7	100	100	5.6	5.6	-0.8	-0.8	100	100	4.9	5.4	-1.4	-1.0
$His_{163}\cdots Tyr_{161}$	100	100	6.3	6.2	-0.7	-0.8	99	100	7.0	6.3	-0.4	-0.7	100	100	6.1	6.6	-0.8	-0.5	100	100	6.8	6.4	-0.5	-0.7
$His_{164}\cdots Pro_{39}$	100	100	4.8	4.8	-1.3	-1.4	100	100	4.9	5.4	-1.4	-1.1	100	100	4.7	4.7	-1.4	-1.4	100	75	4.5	6.3	-1.8	-0.7
$His_{164}\cdots Phe_{181}$	100	100	5.3	5.3	-1.1	-1.2	100	100	5.5	5.6	-1.1	-1.2	100	100	5.2	5.3	-1.2	-1.2	100	92	5.2	6.6	-0.6	-0.6
$His_{164}\cdots Met_{162}$	100	100	5.4	5.3	-1.0	-1.1	98	100	6.0	4.8	-0.7	-1.3	100	100	5.4	5.2	-1.0	-1.1	100	100	5.3	5.1	-1.1	-1.3
$His_{164}\cdots Val_{86}$	100	100	5.9	6.4	-0.7	-0.5	99	96	6.2	6.7	-0.6	-0.4	100	100	6.6	6.6	-0.4	-0.4	100	17	6.2	7.2	-0.6	-0.1

(a) Structural and energetic descriptors of the $Phe_{140}\cdots His_{163}$ and $Phe_{140}\cdots His_{172}$ contacts are particularly affected by the protonation state.

Table S7. Most abundant **enzyme/substrate polar contacts** [(a)] characterized along the last 1.5 μs of the different MD simulations Percentage of abundance (%) and average distances between heavy atoms (*d*) in Å are provided. Subscripts A and B indicates protomers A and B, respectively.

	6LU7_STD				**6LU7_ZW**				**7JUN_STD**				**7JUN_ZW**			
Enzyme···Substrate	$\%_A$	$\%_B$	d_A	d_B	$\%_A$	$\%_B$	d_A	d_B	$\%_A$	$\%_B$	d_A	d_B	$\%_A$	$\%_B$	d_A	d_B
Glu_{166}@O···Ace(P_5)@O (Wat)	55	48	4.2	4.2	11	24	4.1	4.3	56	56	4.2	4.1	26	12	4.3	4.4
Gln_{192}@O···Ala(P_4)@NH	52	39	3.1	3.1	30	60	3.1	3.0	61	62	3.0	3.0	24	--	3.0	--
Thr_{190}@O···Ala(P_4)@O (Wat)	25	55	3.8	4.1	--	57	--	4.4	49	28	3.8	4.1	19	--	5.2	--
Glu_{166}@NH···Val(P_3)@O	**100**	**100**	**3.0**	**3.0**	**46**	**100**	**3.0**	**3.0**	**100**	**100**	**3.0**	**3.0**	**98**	**100**	**3.0**	**3.0**
Glu_{166}@O···Val(P_3)@NH	**99**	**99**	**3.0**	**3.0**	**89**	**100**	**3.0**	**3.0**	**99**	**99**	**3.0**	**3.0**	**99**	**100**	**2.9**	**2.9**
Gly_{143}@NH···Gln(P_1)@O	**99**	**99**	**2.9**	**2.9**	**--**	**99**	**--**	**2.9**	**100**	**100**	**2.9**	**2.9**	**99**	**95**	**2.9**	**3.0**
Cys_{145}@NH···Gln(P_1)@O	12	20	3.2	3.2	--	92	--	3.2	20	--	3.2	--	92	35	3.2	3.2
His_{164}@O···Gln(P_1)@NH	**96**	**95**	**3.1**	**3.1**	**38** [(b)]	**100**	**5.1**	**3.0**	**91**	**90**	**3.1**	**3.1**	**84**[(b)]	**--**	**5.4**	**--**
His_{163}@Nε2H···Gln(P_1)@Oε1	**97**	**99**	**2.9**	**2.9**	**--**	**--**	**--**	**--**	**100**	**99**	**2.9**	**2.9**	**--**	**--**	**--**	**--**
His_{163}@Nε2···Gln(P_1)@Nε2H	--	--	--	--	46	64	3.2	3.1	--	--	--	--	--	95	--	3.1
Phe_{140}@O···Gln(P_1)@Nε2H	**81**	**81**	**3.1**	**3.1**	**20**	**44**	**3.1**	**3.1**	**86**	**92**	**3.1**	**3.0**	**62**	**78**	**3.0**	**3.0**
Glu_{166}@Oε···Gln(P_1)@Nε2H (Wat)	51	48	3.6	3.6	7	15	3.8	4.6	46	48	3.6	3.5	16	8	3.6	4.5
Glu_{166}@Oε···Gln(P_1)@NεH	32	26	3.1	3.1	44	19	2.9	3.0	32	33	3.0	3.0	58	--	2.9	--
Thr_{26}@NH···Ser(P_1')@O	--	--	--	--	--	--	--	--	--	--	--	--	76	7[(b)]	3.0	5.2
His_{41}@O···Ser(P_1')@OγH (Wat)	73	35	4.9	5.1	--	--	--	--	63	92	4.8	4.7	--	8	--	4.3
Thr_{26}@NH···Gly(P_2')@O	56	38	3.1	3.0	--	--	--	--	67	73	3.0	3.1	9	8	3.0	3.1
Asn_{142}@Oδ···Gly(P_2')@NH	--	20	--	3.1	--	78	--	3.0	6	--	3.0	--	78	52	2.9	3.0

[(a)] Data in bold correspond to important contacts that are highly persistent in the **STD** models, but are weakened or lost in the **ZW** ones.

[(b)] Water-mediated contact.

Table S8. Most abundant enzyme/substrate **hydrophobic contacts characterized** along the last 1500 ns of the different MD simulations Percentage of abundance (%), average distances between side chains (*d*) in Å, and interaction energies (*E*) in kcal/mol are provided. Subscripts A and B indicates protomers A and B, respectively.

	6LU7_STD						**6LU7_ZW**						**7JUN_STD**						**7JUN_ZW**					
Enzyme···Substrate	$\%_A$	$\%_B$	d_A	d_B	E_A	E_B	$\%_A$	$\%_B$	d_A	d_B	E_A	E_B	$\%_A$	$\%_B$	d_A	d_B	E_A	E_B	$\%_A$	$\%_B$	d_A	d_B	E_A	E_B
$Leu_{167}\cdots Ala(P_4)$	100	100	4.5	4.6	-0.6	-0.6	53	100	4.6	4.6	-0.6	-0.6	100	100	4.7	4.6	-0.5	-0.6	99	97	4.9	5.3	-0.5	-0.4
$Met_{165}\cdots Ala(P_4)$	100	100	4.1	4.2	-0.6	-0.6	98	99	4.4	4.5	-0.6	-0.5	100	100	4.2	4.2	-0.6	-0.6	99	99	4.5	4.6	-0.6	-0.5
$Phe_{185}\cdots Ala(P_4)$	84	72	5.2	5.1	-0.5	-0.6	45	36	5.0	6.1	-0.6	-0.2	67	78	5.5	5.3	-0.4	-0.5	12	3	6.5	5.5	-0.2	-0.4
$Pro_{168}\cdots Val(P_3)$	11	16	7.2	7.0	-0.2	-0.2	87	9	5.3	7.3	-0.9	-0.2	9	13	7.2	7.2	-0.1	-0.1	50	7	6.4	7.2	-0.4	-0.2
$His_{41}\cdots Leu(P_2)$ [(a)]	**100**	**100**	**4.2**	**4.3**	**-2.0**	**-1.9**	**53**	**56**	**5.7**	**6.9**	**-0.9**	**-0.3**	**100**	**100**	**4.4**	**4.3**	**-1.8**	**-1.9**	**100**	**100**	**4.9**	**5.1**	**-1.3**	**-1.3**
$Met_{165}\cdots Leu(P_2)$	100	100	5.4	5.4	-1.2	-1.1	47	100	5.3	5.3	-1.1	-1.2	100	100	5.4	5.4	-1.2	-1.1	98	100	6.7	5.7	-0.6	-1.0
$Met_{49}\cdots Leu(P_2)$	45	98	5.9	5.3	-0.8	-1.2	52	93	5.6	5.4	-0.9	-1.1	76	6	5.1	6.9	-1.2	-0.5	97	78	6.3	6.1	-0.6	-0.7
$Tyr_{54}\cdots Leu(P_2)$	76	70	7.7	7.8	-0.2	-0.2	5	--	7.8	--	-0.2	--	85	100	7.2	6.8	-0.4	-0.6	3	23	8.2	7.7	-0.1	-0.3
$Met_{49}\cdots Phe(P_3')$	92	24	5.2	6.1	-1.5	-1.0	--	8	--	6.1	--	-1.0	74	99	5.6	4.8	-1.3	-2.0	--	6	--	5.8	--	-1.4

(a) Structural and energetic descriptors of the $His_{41}\cdots Leu(P_2)$ contact are particularly affected by the protonation state.